Biotribology 1–2 (2015) 24–29

Contents lists available at ScienceDirect

Biotribology

journal homepage: http://www.elsevier.com/locate/biotri

Mesh Size Control of Polymer Fluctuation Lubrication in Gemini Hydrogels

Juan Manuel Urueña [a], Angela A. Pitenis [a], Ryan M. Nixon [a], Kyle D. Schulze [a], Thomas E. Angelini [a,b,c], W. Gregory Sawyer [a,d,*]

[a] Department of Mechanical and Aerospace Engineering, University of Florida, Gainesville, FL 32611, United States
[b] J. Crayton Pruitt Family Department of Biomedical Engineering, University of Florida, Gainesville, FL 32611, United States
[c] Institute for Cell Engineering and Regenerative Medicine, University of Florida, Gainesville, FL 32611, United States
[d] Department of Materials Science and Engineering, University of Florida, Gainesville, FL 32611, United States

ARTICLE INFO

Article history:
Received 18 November 2014
Received in revised form 19 February 2015
Accepted 5 March 2015
Available online 12 March 2015

Keywords:
Hydrogel
Polyacrylamide
Friction
Mesh size
Gemini interface
Thermal fluctuations
Polymer physics

ABSTRACT

Polyacrylamide (PAAm) hydrogels are excellent synthetic materials for *in vitro* biotribology studies. Recent work with hydrogels sliding in a Gemini contact has revealed unique friction behavior at low speed that is contrary to the classic Stribeck curve. In these interfaces the friction coefficients are minimum at low speeds and appear to be speed-independent. In this report, we investigate the role of mesh size, ξ, on the low friction regime, termed thermal fluctuation lubrication, and we also explore the origins of a transition from this behavior at higher speeds to polymer relaxation lubrication. PAAm hydrogels of varying concentration were prepared and tested in a Gemini configuration using a pin-on-disk microtribometer with an applied load of 2 mN and over a range of sliding speeds from 0.03 mm/s to 100 mm/s. We found that increasing mesh size or decreasing polymer concentration promotes lower friction coefficients. Many samples underwent a transition from a low friction behavior to an increasing friction coefficient with increasing sliding speed that scaled with speed to the 1/2 power. This transition speed was found to correlate with the mesh size and relaxation time of the polymer network.

1. Introduction

Permeable aqueous materials are ubiquitous in biology, and the tribological study of porous materials in aqueous environments is of great importance to the field of biotribology. In the laboratory, hydrogels are the most common manmade porous materials used in aqueous lubrication studies, while cartilage is the most intensely studied and discussed natural biotribological interface. Despite, decades of experimental and theoretical efforts have aimed at elucidating the lubricating mechanisms of the cartilage system [1–11], and developing a unifying theoretical framework remains elusive. In part this is due to the overwhelming complexity of cartilage and also due to the challenges associated with laboratory measurements of biological tissues. Laboratory studies with hydrogel materials in aqueous environments can complement a large body of work with cartilage or a much more simple system [12–14]. Hydrogels are crosslinked networks of polymer chains that are swollen with water; a representative flexible polymeric hydrogel network is illustrated in Fig. 1. Hydrogels are water-permeable materials, which can be easily created with varying mesh size (ξ), water content, permeability, and elastic properties [15–18].

A central theme in cartilage lubrication is that the cartilage permeability and the shear thinning viscosity of natural synovial fluid work together to provide a thin film of fluid lubrication that separates the surfaces and fully supports the applied load [3,8,11,19–24]. The microstructure of cartilage is nearly universally described as a complex, porous, elastic-solid, and it is often treated as a biphasic material permeated with water [7]. The effective mesh or pore size attributed to cartilage is on the order of 2–6 nm [25]. Synthetic hydrogels are tissue-like in several ways, and the soft, water-permeable character of hydrogels makes them popular biomaterials in tissue engineering applications [26,27]. Unfortunately, there is rarely, if ever, a complete understanding of the tissue that is being mimicked by synthetic hydrogels (*e.g.* the lubrication mechanisms in cartilage).

In tissue engineering and cartilage research, synthetic hydrogels can effectively serve a different, more fundamental purpose, in that they offer a platform from which we can pose and explore theories of lubrication by leveraging the ability to control and characterize nanostructure and carefully examine the role of nanostructure on lubrication [28,18,29–32,17]. Mesh size (ξ) is the single parameter that controls both the elasticity of hydrogels and the dynamics of the constituent polymer chains [33]. All mechanical and transport properties of hydrogels trace back to the mesh size, which is controlled during synthesis by carefully balancing the concentrations of the

* Corresponding author at: Department of Mechanical and Aerospace Engineering, University of Florida, Gainesville, FL 32611, United States. Tel.: +1 352 392 8488; fax: +1 352 392 1071.
E-mail address: wgsawyer@ufl.edu (W. Gregory Sawyer).

http://dx.doi.org/10.1016/j.biotri.2015.03.001
2352-5738/

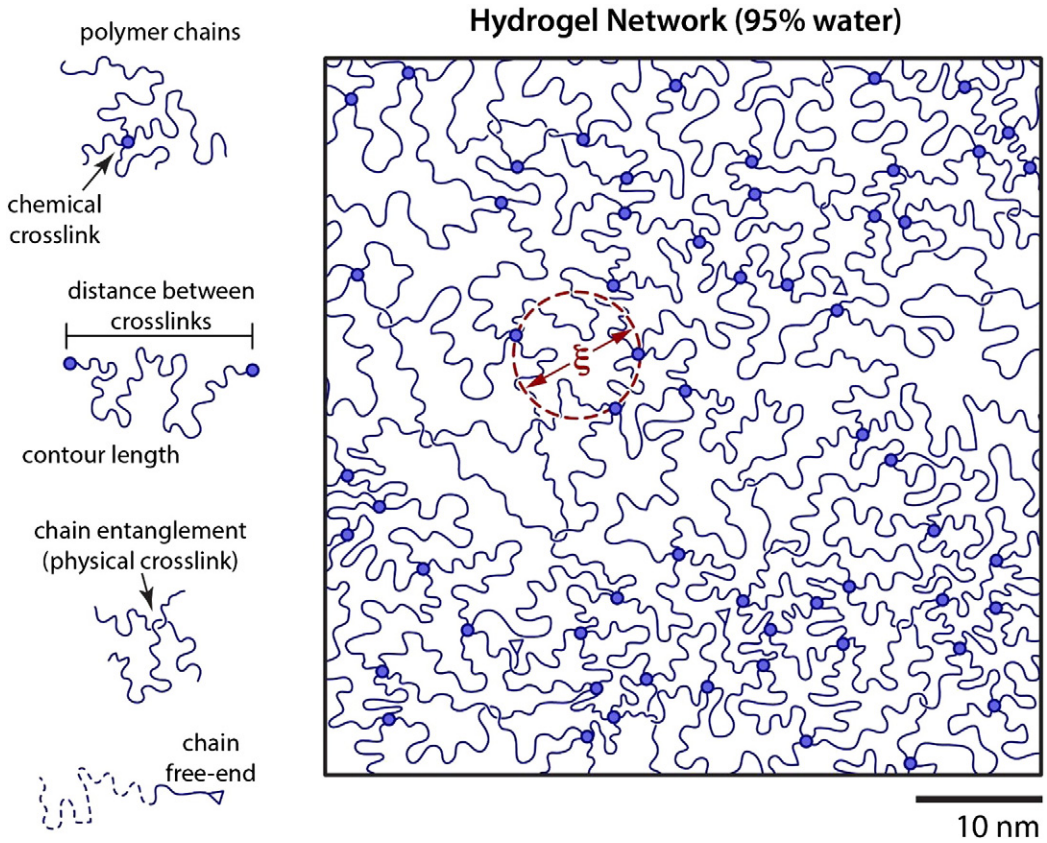

Fig. 1. Illustration of a semi-dilute flexible polymer network, with minimal coil overlap and a persistence length on the order of nanometers. The mesh size (ξ) is approximately 10 nm. This confirms that there are few physical chain entanglements and crosslinking is dominated by chemical crosslinks. Occasionally, polymerization results in freely dangling, uncrosslinked ends indicated here as chain free-ends [59].

monomers and the crosslinking molecules to one another and to water during polymerization [34]. The mesh size is essentially the correlation length between all pairs of molecules comprising the hydrogel network, and in the case of semi-dilute hydrogels made from flexible polymers is of the same order of magnitude as the average spacing between the chemical crosslinks [35]. Occasionally there are physical entanglements, and there may also be unreacted dangling chains that remain after gelation; although both are illustrated in Fig. 1, they are not significant contributors to the physical properties of hydrogels [36].

In this study, we directly examine the role of mesh size on the lubrication mechanisms in self-mated (Gemini) hydrogel interfaces. In previous work on Gemini hydrogel friction, we found that the lubrication curve differed dramatically from the classical engineering Stribeck curve in several major ways [16,37]. First, at slow sliding speeds, where the effects of hydrodynamic lubrication are negligible, Gemini hydrogel friction is actually lowest. Even in the limits of zero sliding speed and startup friction, static friction was remarkably found to be lower than kinetic friction. Second, below a threshold value in speed, this low friction coefficient behavior appears to be speed-independent, but above the transition the friction coefficient rises with Vs 1/2. We hypothesized that the low friction coefficient at low speeds and the transition in friction coefficient at high speeds may be controlled by the polymer network mesh size, ξ, in two different ways: (1) at low speeds through the polymer network elastic modulus, E, and (2) at high speeds with the polymer relaxation time, τ. Both E and τ scale with polymer mesh size raised to the inverse third power, ξ^{-3}, and thus hydrogels of identical chemistry but different mesh size should produce profound changes in both the low-speed friction coefficient and the transition speed.

2. Materials and methods

2.1. Hydrogel preparation

The Gemini hydrogel interface was created by sliding a hydrogel probe against a flat hydrogel disk. Hydrogel probes were made by polymerizing PAAm in a diamond-turned polyolefin mold to produce a probe geometry with ~2 mm radius of curvature. Hydrogel disks were cast in polystyrene Petri dishes to produce sheet geometry with ~60 mm diameter and >4 mm thickness thereby eliminating possible substrate effects.

Hydrogel samples were prepared by synthesizing five different compositions of polyacrylamide (PAAm) hydrogels as shown in Table 1. The acrylamide monomer (AAm) was crosslinked with N, N′-methylenebisacrylamide (MBAm) and catalyzed by a tetramethylethylenediamide (TEMED) reductant and ammonium persulfate (APS) initiator in a solvent of ultrapure water (18.2 MΩ) [38–40]. Aliquots (10–250 g) of each constituent in solution were

Table 1
Constituents of each hydrogel sample reported as percent mass-per-mass of solvent. AAm: acrylamide monomer, MBAm: N,N′-methylenebisacrylamide crosslinker, TEMED: tetramethylethylenediamine catalyst, APS: ammonium persulfate initiator.

Sample no.	AAm	MBAm	TEMED	APS
1	3.75	0.15	0.15	0.15
2	7.50	0.30	0.15	0.15
3	10.00	0.40	0.15	0.15
4	12.50	0.50	0.15	0.15
5	17.50	0.70	0.15	0.15

prepared with a measurement resolution of 1 mg. The ratio of monomer to crosslinking agent was held constant to minimize differences in probe radii of curvature due to swelling. After polymerization, the samples were allowed to equilibrate in ultrapure water for ~40 h prior to experimentation. Scanning white light interferometry was used to determine the surface roughness (Ra) of the probes and sheets after swelling and found to be less than 20 nm.

2.2. Characterization

The mechanical properties of soft, permeable, optically transparent hydrogels are challenging to determine even with *in situ* characterization. Indentation measurements were performed to determine the elastic modulus of the PAAm hydrogel against poly(methyl methacrylate) (PMMA) using the methods and apparatus described in Krick et al. [41]. We revealed the area of contact by implementing particle exclusion microscopy (PEM), wherein the PMMA countersurface was flooded with a solution of monochromatic particles prior to loading a hydrogel probe against the PMMA. The apparent area of contact was determined by observing where particles were excluded from the hydrogel-PMMA interface. A contact diameter of ~1 mm was observed by PEM between the PAAm probe and PMMA sheet under a 2 mN normal force. By this analysis, the Gemini hydrogel interface had a contact pressure of ~3 kPa. Effective contact modulus for each of the five hydrogel samples was calculated for Gemini interfaces from force-displacement curves using the Johnson–Kendall–Roberts (JKR) theory as described in Pitenis et al. The moduli ranged between 1.5–120 kPa, comparable to values found in literature [37,42].

2.3. Swelling

The swelling behavior of PAAm gels in ultrapure water was studied at approximately 20 °C [36,40,43]. Hydrogel samples were cast in a polytetrafluoroethylene (PTFE) tube. After polymerization, each cylindrical sample was extracted and cut in 10–20 mm long sections that were individually placed in ultrapure water in 6 mL glass vials. The sample dimensions were recorded prior to and after ~40 h of swelling. Volume increase was calculated from the difference between the final and initial dimensions, assuming three-dimensional isotropic swelling.

2.4. Small angle X-ray scattering (SAXS)

Small angle X-ray scattering (SAXS) allowed us to characterize the nanoscale structure in the PAAm samples and determine mesh size [44]. We prepared the samples by pipetting the acrylamide mixture, before polymerization, into amorphous quartz capillary tubes of 1.5 mm diameter and 10 μm wall thickness. To enhance Z-contrast between the polymer and solvent, the cured hydrogels were equilibrated against an equal volume of aqueous 100 mM CsCl. The capillaries were flame-sealed and the gels equilibrated overnight before performing SAXS measurements. We collected SAXS data for 10 h per sample on a 2D wire detector with 1024 × 1024 pixels. The 2D $S(q)$ scattering spectra were integrated along the azimuthal direction to produce 1D curves for the entire range of compositions, from 3.75 to 17.5% PAAm, as shown in Fig. 2. By varying composition and fitting the spectra with Lorentzian line-shapes of the form $S(q) = 1/(q^2 + \Gamma^2)$, we determined the mesh size from $\xi = 1/\Gamma$. With increasing polymer content we see a broadening shoulder corresponding to an increase in the Lorentzian width, Γ, and a reduction in mesh size. The reported error bars come from the 95% confidence intervals from non-linear least-squares fitting of the data. We estimate the experimental uncertainty from counting statistics to be approximately the same as the noise seen in the data, approximately 15%, which marginally increases uncertainty of the fitted peak widths.

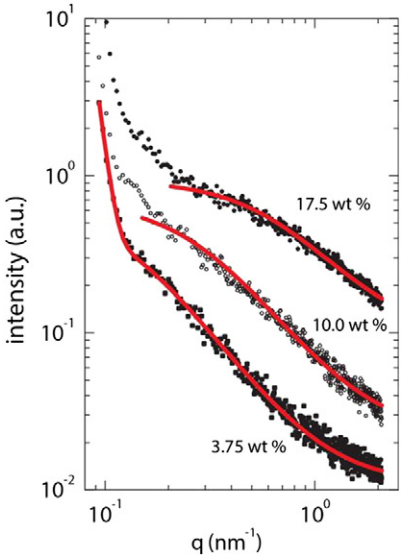

Fig. 2. Scattering spectra show a broadening shoulder at high q with increasing polymer concentration. To measure the width, Γ, showing decreasing ξ with increasing polymer concentration.

2.5. Experimental apparatus

Friction measurements were performed on a high-speed, unidirectional, pin-on-disk microtribometer illustrated in Fig. 3a and described in Pitenis et al. [37]. The PAAm hydrogel probe was molded onto a 4–40 stainless steel set screw and fastened onto a titanium double flexure cantilever assembly with a normal stiffness of 161 μN/μm and a lateral stiffness of 75 μN/μm. The PAAm hydrogel disk was fixed to a piezoelectric rotary stage capable of angular speeds up to 720°/s (Physik Instrumente M-660.55, 4 μrad positional resolution). The stroke radius

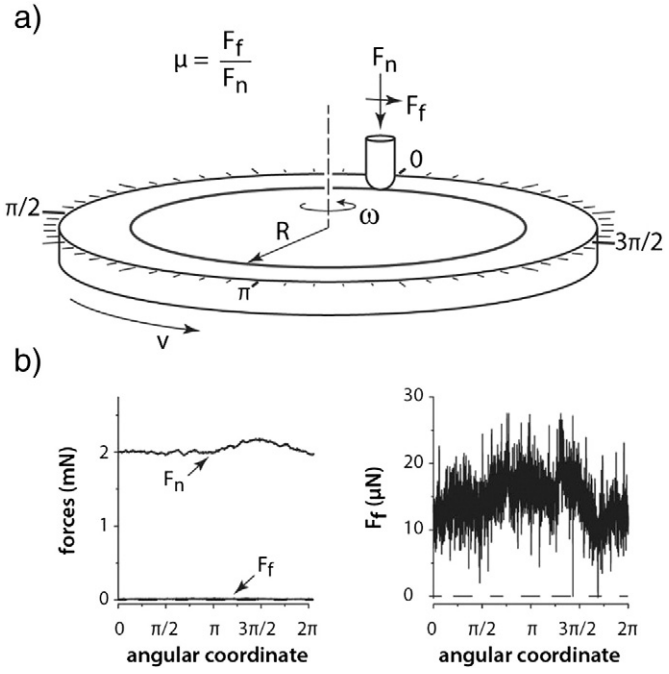

Fig. 3. (a) The Gemini hydrogel configuration consists of a hydrogel probe (4 mm diameter, 2 mm radius of curvature) mounted to a cantilever, slid against a rotating hydrogel disk. (b) Capacitance sensors measure the deflections of the cantilever and output normal (F_n) and friction (F_f) forces. Left: normal and friction forces for a representative cycle (1 revolution). Right: the friction force is two orders of magnitude lower than the normal force.

was 10 mm for sliding speeds of 1–100 mm/s and 1.7 mm for 0.03–0.1 mm/s. The error in friction measurements associated with performing unidirectional pin-on-disk experiments is 0.05% for the 10 mm stroke radius and 30% for the 1.7 mm radius following the analysis in Krick and Sawyer [45]. The hydrogel probe was brought into contact with the hydrogel disk to a normal force of 2 mN by a vertical coarse positioning micrometer stage. The hydrogel probe and hydrogel disk were fully submerged in a bath of ultrapure water during friction experiments. The normal (F_n) and friction (F_f) forces on the probe, shown in Fig. 3b, were measured with 3 mm capacitive displacement sensors (5 μm/V sensitivity and 20 V range) mounted axially and tangentially to the probe, respectively. The friction coefficient, μ, was computed as the ratio of the measured friction force to the normal force.

3. Results and discussion

Gemini hydrogel interfaces can provide exceptionally low friction coefficients under conditions traditionally not thought to promote lubrication, namely, low contact pressure and low sliding speed [16,37]. In the series of experiments described here, the samples with the largest mesh size ($\xi = 9.4 \pm 1.1$ nm) exhibited the lowest measured friction coefficients ($\mu \sim 0.005$), and maintained this behavior over a range of sliding speeds from $V_s = 30$–1000 μm/s. As shown in Fig. 4a, a number of trends emerged, including: (1) friction coefficients decreased with increasing mesh size, (2) friction coefficients were lowest for the slowest sliding speeds, (3) transitions to speed-dependent friction were observed to depend on mesh size, and (4) above the transition speeds, the friction coefficient increased with increasing sliding speed. These trends are captured by a simple scaling law, $\mu = \mu_o + aV_s{}^p$, though the transition regime could not be reached for the hydrogels with the highest polymer concentration and lowest mesh size, as shown in Fig. 4a.

In a hydrogel, the polymer relaxation time is given by $\tau = \xi^3\eta/k_BT$, where ξ is the polymer mesh size, η is the viscosity of water, k_B is the Boltzmann's constant and T is the temperature [35]. We measured mesh size by SAXS finding that for the hydrogels studied here, this relaxation time varies between 5.3×10^{-4} and 0.27 μs. At the surface, characteristic length-scales between polymer chains are roughly equal to the mesh size ξ, and a transition in friction behavior is predicted to occur when the relaxation time, τ, is equal to the time it takes for the surface polymer chains to traverse one mesh size, ξ/V^*. Solving for the transition speed, V^*, gives $V^* = \xi/\tau$ or $V^* = k_BT/\xi^2\eta$. We find, empirically, that this simple scaling law predicts the transition speed, V^*, for all cases in which a transition in friction coefficient behavior is observed.

When the sliding speed, V_s, is rescaled by $V^* = k_BT/\xi^2\eta$ the resulting dimensionless group is $\psi = \xi^2\eta V_s/k_BT$. Remarkably, when the friction coefficient is normalized by μ_o, and plotted *versus* the dimensionless speed parameter, all datasets collapse to a single universal curve (Fig. 4c). The crossover from low-speed to high-speed friction behavior can be mechanistically envisioned as a competition between thermal fluctuations and non-Newtonian shear. At low speeds, the non-Newtonian shear effects are negligible and thermal fluctuation

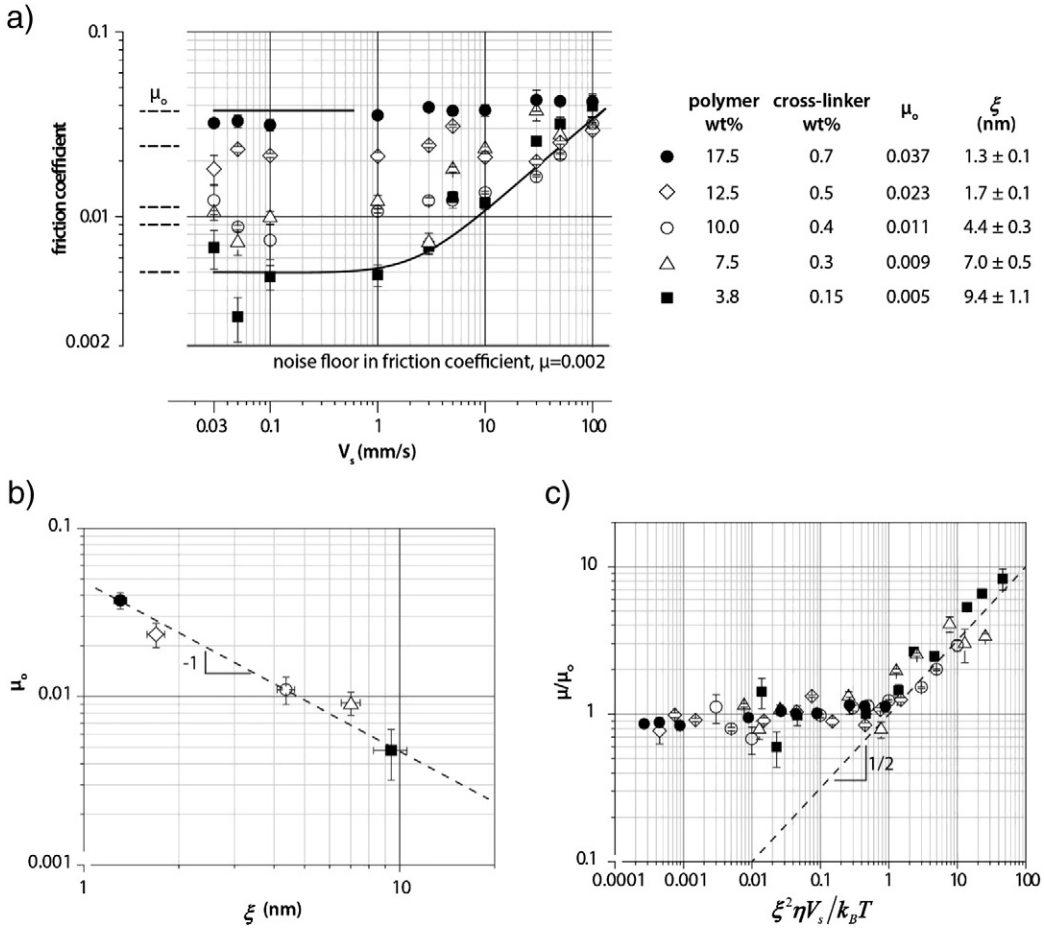

Fig. 4. (a) Friction coefficient as a function of sliding speed for five different polymer concentrations. Solid lines are guides that highlight the transition in friction behavior as the sliding speed increases. The horizontal dashed lines are fits to the friction coefficient in the speed-independent regime, μ_o, for each of the five samples. Polymer concentration and crosslinker reported as weight percent, μ_o, and mesh size, ξ, are tabulated in the legend. (b) Friction coefficient in the speed-independent regime (μ_o) scales with mesh size to -1 power. (c) Collapsing the data in (a) results in a universal curve that illustrates the transition in friction behavior between the speed-independent and the speed-dependent friction regimes. In the speed-dependent regime, normalized friction coefficient scales with 1/2 power.

processes likely dominate the lubrication mechanism. Conversely, at high speeds the dominant process involves non-Newtonian mechanics of shearing across the sliding interface and the passing frequencies of the surface chains exceed the fluctuation frequencies. Interestingly, the friction coefficient in the speed-independent regime, μ_o, and the transition speed, V^*, both increase with increasing polymer concentration or decreasing mesh size. Neither the friction behavior nor simple hydrodynamic lubrication equations support a hypothesis that these transitions are in any way related to the onset of fluid films [46]. To our knowledge the mathematical treatment of fluid lubrication across permeable interfaces has not been solved, but we expect that permeability will reduce the fluid film thickness. We suggest that all of these sliding experiments involve the contact across the sliding interfaces. A plot of the friction coefficient in the speed-independent regime, μ_o, *versus* mesh size, ξ, shows a roughly hyperbolic scaling (Fig. 4b).

The scaling of μ_o with ξ provides clues about the origins of mesh size dependent friction. Hydrogels with increased polymer concentration have a smaller mesh size, so it is sensible to hypothesize that friction coefficient should increase linearly with the number of polymer chains accessible to direct contact at the interface, $\mu_o \sim Ac_s$, where A is contact area and c_s is polymer surface concentration — the number of polymers at the surface per unit area. For a fixed normal load and indentation radius of curvature, $F_n = 2$ mN and $R = 2$ mm in our experiments, the contact area will vary depending on the hydrogel elastic modulus, E. Using the Hertz force-indentation relation, the scaling between contact area and elastic modulus is $A \sim E^{-2/3}$. The elastic modulus of a semi-dilute hydrogel composed of flexible polymers scales with network mesh size like $E \sim \xi^{-3}$. The lowest-order estimate of the scaling between mesh size and surface concentration is $c_s \sim \xi^{-2}$, where doubling the linear length-scale, ξ, quadruples the characteristic area per mesh. The resulting prediction for friction coefficient is then $\mu_o \sim \xi^2\xi^{-2} = \xi^0$. A more careful treatment following the analysis presented by de Gennes[†] predicts $c_s \sim \xi^{-8/9}$, and $\mu_o \sim \xi^2\xi^{-8/9} = \xi^{10/9}$ [35]. Both predictions show that the hydrogel modulus scales so strongly with mesh size, compared to surface chain concentration, that the effects of contact area compensate or dominate the effects of surface chain density. Neither prediction captures our measurements of μ_0 *versus* ξ qualitatively, suggesting that the dominant frictional mechanism is not merely chain–chain contact.

In equilibrium, the mesh size is determined by the statistical mechanics of chain fluctuations. Much like the Flory radius, R_f, or more generally speaking, the RMS end-to-end distance for free chains, the mesh size is not only a characteristic structural length-scale, but is also approximately the amplitude of dynamic chain fluctuation [35]. Thus polymer chains at a hydrogel surface of larger mesh size will fluctuate with increased amplitudes. The random thermal fluctuations of polymers at the Gemini interface rapidly relax shear strain generated during sliding, and, similar to the mechanism underlying thermolubricity [47], provide a blurred interface over which the barriers to sliding are effectively reduced. The reciprocal scaling of low speed friction coefficient, μ_0, with ξ highlights the dominating effect of polymer fluctuation amplitude in frictional interactions at the Gemini interface. Moreover, it is interesting to note that extrapolating our measurements to a mesh size of only a few Å, which would describe a solid PMMA material with minimal dynamic fluctuations, gives $\mu_0 = 0.8$, consistent with dry sliding friction.

Gemini hydrogel friction behavior both resembles and differs from the lubrication of self-mated solvated polymer brushes [48–50,15]. Previous studies of polymer brushes measured in a surface force apparatus (SFM) have shown that at low speeds (~450 nm/s) these materials achieved extremely low friction coefficients ($\mu < 0.001$) by polymer chain fluctuations [51]. In 2011, Nomura et al. used an AFM-colloidal probe technique to show a transition in friction coefficient from $\mu < 0.001$ at low shear rates (1–10 μm/s) to $\mu \sim 0.01$ at higher shear rates (10^3 μm s^{-1}) between polystyrene brushes in toluene [52]. However, when the polymer brush interface is measured in a macrotribometer, the resulting lubrication curve resembles the classic Stribeck curve at speeds above 1 mm s^{-1} [53]. Furthermore, at mN normal loads, the contact pressure at the polymer brush interface is orders of magnitude greater than the Gemini hydrogel interface, which provides an important point of distinction between the two materials [51].

The ease with which hydrogels are synthesized and molded makes a vast breadth of tunable parameters and physical processes accessible to experiments, facilitating studies without the challenges that come with measuring real tissue samples, whether performed *in vivo* or *ex vivo*. Natural lubricating surfaces are usually made from semi-dilute networks of flexible anionic polymers, including proteoglycans like lubricin or glycosaminoglycans like hyaluronic acid and mucin [54]. These networks may be stabilized by multivalent cationic counterions or cationic proteins, like Ca^{2+} and lysozyme, which act like ionic crosslinkers [55]. In the outer layers of cartilage, the mesh size of these networks is approximately 2–6 nm, which lies within the range of mesh sizes tested here with PAAm gels [25]. Thus, it is intriguing that the low-speed friction coefficient of PAAm, μ_0, is found to be the same as typically reported for cartilage, between 0.01 and 0.02 [3]. If the underlying mechanisms of hydrogel friction shown here also apply to tissue, we predict that a transition to higher friction coefficient will occur *in vivo* between 10 and 100 mm/s, controlled by the polymer relaxation time. The rate that the eyelid slides past the cornea during a blink as well as the upper limit on sliding speeds in articulating joints falls within this range. Considering the conformal geometries, numerical simulations suggest that hydrodynamic lubrication should separate the surfaces above ~100 mm/s [56–58]. In the future, using hydrogels as highly controllable tissue mimics, we can explore the role of polymer charge density and fluid viscosity in hydrogel friction to draw further connections between tissue and hydrogels. The range of sliding speed will be increased further as well, exploring friction at startup and searching for a high-speed transition from polymer relaxation lubrication into hydrodynamic lubrication. The continued development of new basic scaling laws relating friction to polymer physics through the study of model hydrogel systems aims to one day build a unifying framework from which we can interpret biological lubrication.

3.1. Concluding remarks

Gemini hydrogel frictional behavior exhibits two lubrication regimes within the four orders of magnitude in sliding speed explored here. In contrast to classical lubrication regimes, here we measure the lowest friction coefficient at the lowest sliding speeds.

We do not attribute these distinct regimes to fluid film lubrication. Rather, we associate them with polymer fluctuation at the surface.

The transition point is consistent with a model of rapidly fluctuating polymer chains that are experiencing repeated sliding contacts, whereby the period between contacts is defined by the mesh size divided by the sliding speed. Given knowledge of the polymer relaxation times, the transition speed becomes $V^* = k_BT/\xi^2\eta$ and the transition criterion becomes $\xi^2\eta V_s/k_BT = 1$.

Conflict of interest

The authors declare that there are no conflicts of interest.

Acknowledgments

This work was supported by Alcon Laboratories.

[†] The classic treatments of semi-dilute gels of flexible polymers show that mesh size scales with volumetric polymer concentration like $\xi \sim c^{-3/4}$. The conversion between surface concentration and bulk concentration, ignoring geometric factors, is $c_s \sim c^{2/3}$. So, in this treatment, the mesh size scales with surface concentration as $c_s \sim \xi^{-8/9}$ [35].

References

[1] Jones ES. Joint lubrication. Lancet 1936;227:1043–5. http://dx.doi.org/10.1016/S0140-6736(01)37157-X.
[2] Charnley J. The lubrication of animal joints. Symp Biomech 1959:12–22.
[3] Lewis PR, McCutchen CW. Mechanism of animal joints: experimental evidence for weeping lubrication in mammalian joints. Nature 1959;184:1284–5. http://dx.doi.org/10.1038/1841285a0.
[4] McCutchen CW. The frictional properties of animal joints. Wear 1962;5:1–17. http://dx.doi.org/10.1016/0043-1648(62)90176-X.
[5] McCutchen CW. Lubrication of joints. The Joints and Synovial Fluid. New York: Academic Press; 1978 437–83.
[6] Little K, Freeman MAR, Swanson SAV. Experiments on friction in the human hip joint. In: Wright V, editor. Lubr. Wear Joints. London: Sector; 1969. p. 110–6.
[7] Mow VC, Kuei SC, Lai WM, Armstrong CG. Biphasic creep and stress relaxation of articular cartilage in compression: Theory and experiments. J Biomech Eng 1980;102:73–84.
[8] Forster H, Fisher J. The influence of loading time and lubricant on the friction of articular cartilage. Proc Inst Mech Eng H J Eng Med 1996;210:109–19.
[9] Schmidt TA, Gastelum NS, Nguyen QT, Schumacher BL, Sah RL. Boundary lubrication of articular cartilage: role of synovial fluid constituents. Arthritis Rheum 2007;56:882–91. http://dx.doi.org/10.1002/art.22446.
[10] Accardi MA, Dini D, Cann PM. Experimental and numerical investigation of the behaviour of articular cartilage under shear loading—interstitial fluid pressurisation and lubrication mechanisms. Tribol Int 2011;44:565–78. http://dx.doi.org/10.1016/j.triboint.2010.09.009.
[11] Moore AC, Burris DL. An analytical model to predict interstitial lubrication of cartilage in migrating contact areas. J Biomech 2014;47:148–53. http://dx.doi.org/10.1016/j.jbiomech.2013.09.020.
[12] Buwalda SJ, Boere KWM, Dijkstra PJ, Feijen J, Vermonden T, Hennink WE. Hydrogels in a historical perspective: from simple networks to smart materials. J Control Release 2014;190:254–73. http://dx.doi.org/10.1016/j.jconrel.2014.03.052.
[13] Sardinha VM, Lima LL, Belangero WD, Zavaglia C, Bavaresco VP, Gomes JR. Tribological characterization of polyvinyl alcohol hydrogel as substitute of articular cartilage. Wear 2013;301:218–25. http://dx.doi.org/10.1016/j.wear.2012.11.054.
[14] Kirschner CM, Anseth KS. Hydrogels in healthcare: from static to dynamic material microenvironments. Acta Mater 2013;61:931–44. http://dx.doi.org/10.1016/j.actamat.2012.10.037.
[15] Tokita M, Tanaka T. Friction coefficient of polymer networks of gels. The Journal of Chemical Physics 1991;95:4613–9. http://dx.doi.org/10.1063/1.461729.
[16] Dunn AC, Sawyer WG, Angelini TE. Gemini interfaces in aqueous lubrication with hydrogels. Tribol Lett 2014;54:59–66. http://dx.doi.org/10.1007/s11249-014-0308-1.
[17] Gong JP. Friction and lubrication of hydrogels its richness and complexity. Soft Matter 2006;2:544. http://dx.doi.org/10.1039/b603209p.
[18] Gong JP, Kurokawa T, Narita T, Kagata G, Osada Y, Nishimura G, et al. Synthesis of hydrogels with extremely low surface friction. J Am Chem Soc 2001;123:5582–3. http://dx.doi.org/10.1021/ja003794q.
[19] Radin EL, Paul IL, Pollock D. Animal joint behaviour under excessive loading. Nature 1970;226:554–5. http://dx.doi.org/10.1038/226554a0.
[20] Krishnan R, Kopacz M, Ateshian GA. Experimental verification of the role of interstitial fluid pressurization in cartilage lubrication. J Orthop Res 2004;22:565–70. http://dx.doi.org/10.1016/j.orthres.2003.07.002.
[21] Bonnevie ED, Baro V, Wang L, Burris DL. In-situ studies of cartilage microtribology: roles of speed and contact area. Tribol Lett 2011;41:83–95. http://dx.doi.org/10.1007/s11249-010-9687-0.
[22] Bonnevie ED, Baro VJ, Wang L, Burris DL. Fluid load support during localized indentation of cartilage with a spherical probe. J Biomech 2012;45:1036–41. http://dx.doi.org/10.1016/j.jbiomech.2011.12.019.
[23] Park S, Krishnan R, Nicoll SB, Ateshian GA. Cartilage interstitial fluid load support in unconfined compression. J Biomech 2003;36:1785–96. http://dx.doi.org/10.1016/S0021-9290(03)00231-8.
[24] Ateshian GA. The role of interstitial fluid pressurization in articular cartilage lubrication. J Biomech 2009;42:1163–76. http://dx.doi.org/10.1016/j.jbiomech.2009.04.040.
[25] Mow VC, Ratcliffe A, Robin Poole A. Cartilage and diarthrodial joints as paradigms for hierarchical materials and structures. Biomaterials 1992;13:67–97. http://dx.doi.org/10.1016/0142-9612(92)90001-5.
[26] Ratner BD, Hoffman AS. Hydrogels for Medical and Related Applications, vol. 31Washington, D. C.: American Chemical Society; 1976. http://dx.doi.org/10.1021/bk-1976-0031.
[27] Peppas NA, Bures P, Leobandung W, Ichikawa H. Hydrogels in pharmaceutical formulations. European Journal of Pharmaceutics and Biopharmaceutics 2000;50:27–46. http://dx.doi.org/10.1016/S0939-6411(00)00090-4.
[28] Gong JP, Osada Y. Gel friction: A model based on surface repulsion and adsorption. J Chem Phys 1998;109:8062. http://dx.doi.org/10.1063/1.477453.
[29] Gong JP, Osada Y. Surface friction of polymer gels. Prog Polym Sci 2002;27:3–38. http://dx.doi.org/10.1016/S0079-6700(01)00037-5.
[30] Osada Y, Gong J-P. Soft and wet materials: polymer gels. Adv Mater 1998;10:827–37. http://dx.doi.org/10.1002/(SICI)1521-4095(199808)10:11<827::AID-ADMA827>3.0.CO;2-L.
[31] Gong J, Higa M, Iwasaki Y, Katsuyama Y, Osada Y. Friction of gels. J Phys Chem B 1997;101:5487–9. http://dx.doi.org/10.1021/jp9713118.
[32] Kaneko D, Tada T, Kurokawa T, Gong JP, Osada Y. Mechanically strong hydrogels with ultra-low frictional coefficients. Adv Mater 2005;17:535–8. http://dx.doi.org/10.1002/adma.200400739.
[33] Zhang J, Peppas NA. Synthesis and Characterization of pH- and Temperature-Sensitive Poly(Methacrylic Acid)/Poly(N-isopropylacrylamide) Interpenetrating Polymeric Networks; 2000 102–7.
[34] Brannon-Peppas L. Absorbent Polymer Technology, vol. 8Elsevier; 1990. http://dx.doi.org/10.1016/B978-0-444-88654-5.50008-X.
[35] De Gennes P-G. Scaling Concepts in Polymer Physics. Cornell University Press; 1979.
[36] Gehrke S. Synthesis, equilibrium swelling, kinetics, permeability and applications of environmentally responsive gels. Responsive Gels Vol Transitions II 1993. http://dx.doi.org/10.1007/BFb0021130 %I.
[37] Pitenis AA, Urueña JM, Schulze KD, Nixon RM, Dunn AC, Krick BA, et al. Polymer fluctuation lubrication in hydrogel gemini interfaces. Soft Matter 2014. http://dx.doi.org/10.1039/C4SM01728E.
[38] Billmeyer FW. Textbook of Polymer Science. 3rd ed. New York: John Wiley & Sons; 1984.
[39] Sperling LH. Introduction to Physical Polymer Science. 4th ed. Wiley—Interscience; 2005.
[40] Mathur AM, Moorjani SK, Scranton AB. Methods for synthesis of hydrogel networks: a review. J Macromol Sci C Polym Rev 1996;36:405–30. http://dx.doi.org/10.1080/15321799608015226.
[41] Krick BA, Vail JR, Persson BNJ, Sawyer WG. Optical in situ micro tribometer for analysis of real contact area for contact mechanics, adhesion, and sliding experiments. Tribol Lett 2011;45:185–94. http://dx.doi.org/10.1007/s11249-011-9870-y.
[42] Yeung T, Georges PC, Flanagan LA, Marg B, Ortiz M, Funaki M, et al. Effects of substrate stiffness on cell morphology, cytoskeletal structure, and adhesion. Cell Motil Cytoskeleton 2005;60:24–34. http://dx.doi.org/10.1002/cm.20041.
[43] Saraydın D, Karadag˘ E, Işıkver Y, Şahiner N, Güven O. The influence of preparation methods on the swelling and network properties of acrylamide hydrogels with crosslinkers. J Macromol Sci A 2004;41:419–31. http://dx.doi.org/10.1081/MA-120028476.
[44] Mallam S. Scattering and swelling properties. Macromolecules 1989;22:3356–61.
[45] Krick BA, Sawyer WG. A little analysis of errors in friction for small wear tracks. Tribol Lett 2010;39:221–2. http://dx.doi.org/10.1007/s11249-010-9605-5.
[46] Hamrock BJ, Schmid SR, Jacobson BO. Fundamentals of fluid film lubrication. 2nd ed. CRC Press; 2004.
[47] Jinesh K, Krylov S, Valk H, Dienwiebel M, Frenken J. Thermolubricity in atomic-scale friction. Phys Rev B 2008;78:155440. http://dx.doi.org/10.1103/PhysRevB.78.155440.
[48] Perrino C, Lee S, Spencer ND. End-grafted sugar chains as aqueous lubricant additives: synthesis and macrotribological tests of poly(l-lysine)-graft-dextran (PLL-g-dex) copolymers. Tribol Lett 2009;33:83–96. http://dx.doi.org/10.1007/s11249-008-9402-6.
[49] Lee S, Müller M, Heeb R, Zürcher S, Tosatti S, Heinrich M, et al. Self-healing behavior of a polyelectrolyte-based lubricant additive for aqueous lubrication of oxide materials. Tribol Lett 2006;24:217–23. http://dx.doi.org/10.1007/s11249-006-9121-9.
[50] Lee S, Müller M, Ratoi-Salagean M, Vörös J, Pasche S, Paul SM De, et al. Boundary Lubrication of Oxide Surfaces by Poly(L-lysine)-g-poly(ethylene glycol) (PLL-g-PEG) in Aqueous Media. Tribol Lett n.d.;15:231–9. doi:10.1023/A:1024861119372.
[51] Klein J, Kumacheva E, Mahalu D, Perahia D, Fetters LJ. Reduction of frictional forces between solid surfaces bearing polymer brushes. Nature 1994;370:634–6. http://dx.doi.org/10.1038/370634a0.
[52] Nomura A, Okayasu K, Ohno K, Fukuda T, Tsujii Y. Lubrication mechanism of concentrated polymer brushes in solvents: effect of solvent quality and thereby swelling state. Macromolecules 2011;44:5013–9. http://dx.doi.org/10.1021/ma200340d.
[53] Nalam PC, Clasohm JN, Mashaghi A, Spencer ND. Macrotribological studies of poly(L-lysine)-graft-poly(ethylene glycol) in aqueous glycerol mixtures. Tribol Lett 2010;37:541–52. http://dx.doi.org/10.1007/s11249-009-9549-9.
[54] Jay GD, Torres JR, Warman ML, Laderer MC, Breuer KS. The role of lubricin in the mechanical behavior of synovial fluid. Proc Natl Acad Sci U S A 2007;104:6194–9. http://dx.doi.org/10.1073/pnas.0608558104.
[55] Sanders L, Guáqueta C, Angelini T, Lee J-W, Slimmer S, Luijten E, et al. Structure and stability of self-assembled actin-lysozyme complexes in salty water. Phys Rev Lett 2005;95:108302. http://dx.doi.org/10.1103/PhysRevLett.95.108302.
[56] Nairn JA, City SL, Jiang T. Measurement of the Friction and Lubricity Properties of Contact lenses Friction and Lubricity Apparatus; 1995 1–5.
[57] Hung G, Hsu F, Stark L. Dynamics of the human eyeblink. Am J Optom Physiol Opt 1977;54:678–90.
[58] Pascovici MD, Cicone T. Squeeze-film of unconformal, compliant and layered contacts. Tribol Int 2003;36:791–9. http://dx.doi.org/10.1016/S0301-679X(03)00095-1.
[59] Grillet AM, Wyatt NB, Gloe LM. Polymer gel rheology and adhesion. In: De Vicente J, editor. Rheology, InTech; 2012. p. 59–80. http://dx.doi.org/10.5772/2065.